

# A comparison of ancient deltaic shoreline progradation with modern deltaic progradation rates: Unravelling the temporal structure of the shallow-marine Blackhawk Formation, Upper Cretaceous Western Interior Seaway, USA

Tore Aadland<sup>1,2</sup>  | Gary Hampson<sup>3</sup>  | William Helland-Hansen<sup>1</sup> 

<sup>1</sup>Department of Earth Science, University of Bergen, Bergen, Norway

<sup>2</sup>Research Centre for Arctic Petroleum Exploration, University of Tromsø, Tromsø, Norway

<sup>3</sup>Department of Earth Science & Engineering, Imperial College London, London, UK

## Correspondence

Gary Hampson, Department of Earth Science & Engineering, Imperial College London, London SW7 2AZ, UK.  
Email: [g.j.hampson@imperial.ac.uk](mailto:g.j.hampson@imperial.ac.uk)

## Funding information

ARCEX; Norges Forskningsråd, Grant/Award Number: 228107

## Abstract

Understanding how sedimentary rocks represent time is one of the significant challenges in sedimentology. Sedimentation rates retrieved from vertical sections are strongly timescale dependent, which means that we cannot use empirical rate data derived from vertical sections in modern environments to interpret the temporal structure of ancient sedimentary deposits. We use the Lower to Middle Campanian Blackhawk Formation deposits in eastern Utah and western Colorado as a natural laboratory to test a source-to-sink methodology circumventing this timescale dependence by relating modern progradation rates to the deltaic shoreline progradation of ancient siliciclastic rocks. Our objective is to quantify how much time is needed to account for the observed cumulative deltaic shoreline progradation recorded by the shallow-marine sandstone bodies of the Blackhawk Formation in terms of progradation rates derived from comparable modern deltaic systems. By making the simplifying assumption that the Blackhawk Formation rocks were deposited along a linear coastline that only grew by aggradation and progradation, it is possible to argue that the stratigraphic completeness of two-dimensional dip-oriented stratigraphic cross-sections through these deposits should be high. Furthermore, we hypothesise that delta progradation estimates capture a significant portion of the biostratigraphically and radiometrically constrained duration of the succession. By comparing the recorded progradation with modern progradation rates, we estimate that we need ca. 20% (median value, with minimum and maximum estimates of 2% and 300%) of the time available from biostratigraphic and radiometric dating to account for the progradation recorded by the sedimentary deposits. This indicates that long-term progradation rates averaged over the entire duration of the Blackhawk Formation were only a factor of five times slower than the modern progradation rates derived from observations

This is an open access article under the terms of the [Creative Commons Attribution-NonCommercial-NoDerivs](https://creativecommons.org/licenses/by-nc-nd/4.0/) License, which permits use and distribution in any medium, provided the original work is properly cited, the use is non-commercial and no modifications or adaptations are made.

© 2022 The Authors. *Basin Research* published by International Association of Sedimentologists and European Association of Geoscientists and Engineers and John Wiley & Sons Ltd.

over periods that are five to six orders of magnitude shorter. We conclude that a significant amount of time is represented by prograding deltaic shoreline deposits and that by considering the cumulative shoreline progradation, we could limit the effects of timescale dependence on the rate estimates used in our analysis.

#### KEYWORDS

Blackhawk Formation, progradation rate, source-to-sink, temporal structure, trajectory analysis

## 1 | INTRODUCTION

Understanding the temporal structure of sedimentary rocks is a significant challenge in sedimentology. Empirically derived sedimentation rates from vertical sections are inversely correlated with the duration over which the rates are sampled (Miall, 2015; Reineck, 1960; Sadler, 1981; Sadler & Jerolmack, 2015; Schindel, 1980). This timescale dependence implies that we cannot directly use empirical data derived from modern environments when interpreting depositional rates and duration of basin filling of ancient sedimentary deposits (e.g. Miall, 2015).

A recent finding by Sadler and Jerolmack (2015) is that the timescale dependence of vertical aggradation rates (Miall, 2015; Reineck, 1960; Sadler, 1981; Sadler & Jerolmack, 2015; Schindel, 1980) may be due to the progradational component of sediment accumulation not being satisfactorily accounted for. They also demonstrated that accumulation rates measured from two-dimensional sections are less timescale dependent than their one-dimensional vertical components. Similarly, Mahon et al. (2015) showed that successions with prograding clinoforms had significantly higher stratigraphic completeness than one-dimensional stratigraphic sections. These findings are consistent with the notion that measurements of sedimentation over more dimensions and larger regions record the transition from localised, episodic processes (e.g. stochastic and autogenic landscape dynamics) to integrated, more uniform patterns (e.g. basin-scale interplay between sediment supply and accommodation) (Hajek & Straub, 2017; Straub et al., 2020; Wang et al., 2011).

Aadland et al. (2018) presented a model that linked the timescale dependency of sedimentation rates to the dimensionality of the rate estimates, which means that timescale-dependent sediment accumulation rates can arise as an effect of the square-cube law; a mathematical principle that emphasises the non-linear relationship between the volumes and surface areas of growing objects. Significantly, the model of Aadland et al. (2018) provides a framework by which to attribute variable stratigraphic completeness to this dimensionality effect.

### Highlights

1. We test a model that links the timescale dependency of sedimentation rates to the dimensionality of the rate estimates by relating modern progradation rates to ancient strata that record deltaic shoreline progradation.
2. Our test is carried out using data from the well documented, shallow-marine Blackhawk Formation.
3. Long-term progradation rates averaged over the entire duration of the Blackhawk Formation were only a factor of five times slower than the modern progradation rates derived from observations over periods that are five to six orders of magnitude shorter.
4. By considering the cumulative shoreline progradation, we could limit the effects of timescale dependence on sedimentation rate estimates. This approach provides a new source-to-sink tool for basin analysis.

In this study, we (i) quantify the progradation rate of the Blackhawk Formation wave-dominated deltaic shorelines using the source-to-sink methodology outlined in Aadland and Helland-Hansen (2019) and subsequently the time captured in the formation, and (ii) assess the discrepancy between these time estimates, and the time estimates constrained from biostratigraphic and radiometric data in the formation.

A source-to-sink analysis is an approach to sedimentological and stratigraphic analysis that attempts to give a holistic understanding of the entire depositional system, including the sediment source and the sediment routing system (Allen, 2017; Helland-Hansen et al., 2016; Nyberg et al., 2018; Romans et al., 2016). Two different modes of sediment transport characterise the transfer of sediment to the depositional sinks by fluvial systems: suspended load (dominated by grain sizes of silt and finer) and bedload (dominated by grain sizes of sand and coarser) (Turowski et al., 2010). About 90% of the sediment delivered to the

world's oceans by fluvial systems is delivered as suspended load (Syvitski & Milliman, 2007), and this forms mud-dominated sedimentary blankets in the offshore and deep-water domains. Mud-dominated suspended load is more mobile than its sandy counterpart and is easily dispersed significant distances away from fluvial entry points by oceanic circulation (Cattaneo et al., 2003; Patruno et al., 2015; Yang & Liu, 2007).

Sediment production models applied in source-to-sink studies focus predominantly on the suspended sediment load component of sediment transport as reflected in the BQART model of Syvitski and Milliman (2007) and its precursor (Syvitski et al., 2003, 2005), and the RoBART model of Nyberg et al. (2021). In contrast, for bedload, there are no sediment production models that estimate the rate and volume of upstream transport that can feasibly be applied to the study of ancient deposits (Nyberg et al., 2021).

An approach to circumvent the lack of bedload models was suggested by Aadland and Helland-Hansen (2019). They quantified the progradation rates of deltaic bedload material (typically sand) using satellite images acquired in the period 1984 to 2015 and presented a model of modern deltaic progradation rates that takes fluvial water discharge and suspended sediment load as input. Using this model, it is possible to analyse deltaic shoreline progradation without constraining bedload transport rates.

This paper considers the wave-dominated deltaic and shoreface sandstones of the Upper Cretaceous Blackhawk Formation, central Utah, USA. The Blackhawk Formation represents a natural laboratory rich in outcrop and subsurface data in which it is possible to test new ideas and methodologies for analysing siliciclastic depositional systems. In particular, the rocks are comprised of the appropriate type of depositional facies for our approach, they consist of stratigraphic units and horizons that can be mapped over large distances, and the succession has experienced only minor modification by post-depositional tectonic processes (e.g. Balsley, 1980; Hampson, 2010; Kamola & Van Wagoner, 1995; Pattison, 2020; Van Wagoner, 1995; Young, 1955).

It should be noted that the method proposed in Aadland and Helland-Hansen (2019) more strongly reflects fluvio-deltaic processes than basinal processes and that fluvial processes in the wave-dominated shallow-marine Blackhawk Formation therefore may have been underestimated relative to basinal processes. This may introduce some ambiguity in the results, but we justify this approximation given the first-order nature of our approach. As for other ancient sedimentary rocks, the temporal constraints are relatively limited; the highest resolution obtained is by the relative dating of ammonite biozones.

We are interested in exploring how the temporal aspects of the cumulative deltaic shoreline progradation

recorded within the Blackhawk Formation compare with the progradation rates of modern deltaic systems. If the area prograded and the 'available' time-constraint for progradation as determined by biostratigraphic and radiometric data is consistent with the modern progradation rates, it may indicate that it is feasible to use models of modern progradation rate as a tool to predict the temporal structure of ancient deltaic deposits. On the contrary, if there is a significant discrepancy between the 'available' time and the time needed to account for the observed progradation, it indicates that the proposed methodology is flawed. A likely explanation of this would be that the analysis performed does not satisfactorily account for the timescale dependency of the sediment accumulation investigated. Here we assume that the Blackhawk Formation was deposited with a linear coastline that grew by aggradation and progradation. This is significant because the geometric model of timescale dependency on sedimentation rates presented in Aadland et al. (2018) predicts that the stratigraphic completeness of two-dimensional dip-oriented stratigraphic cross-sections through such deposits should be high.

The objective of this paper is to explore, by applying the source-to-sink-based progradation rate model of Aadland and Helland-Hansen (2019), how much time is captured by deltaic shoreline progradation within the Blackhawk Formation by comparing the area of shoreline migration recorded within the formation with progradation rates derived from comparable modern deltaic systems. By doing this, we apply for the first time the concept of timescale dependency being linked to the dimensionality of rate estimates to an outcrop section to show that a significant portion of time-constrained by biostratigraphy can be accounted for.

## 2 | GEOLOGICAL OVERVIEW

The Lower to Middle Campanian Blackhawk Formation of the Mesaverde Group in eastern Utah and western Colorado, USA (Figure 1) is exceptionally well exposed across large areas (e.g. Balsley, 1980; Pattison, 2020; Van Wagoner, 1995; Young, 1955), exemplified by two high-quality, nearly shoreline-perpendicular continuous outcrop sections 200 and 300 km long (cf. figs. 4 and 5 in Hampson, 2010). In addition, the strata are penetrated by over 2800 wells. This makes it possible to determine the sedimentological characteristics and stratigraphic architecture of the formation over 60,000 km<sup>2</sup>. The strata represent a complete depositional system comprising fluvial, deltaic, and offshore deposits arranged in compound clinofolds consisting of a sandstone-dominated fluvial-to-shoreface clinofold and a mudstone-dominated

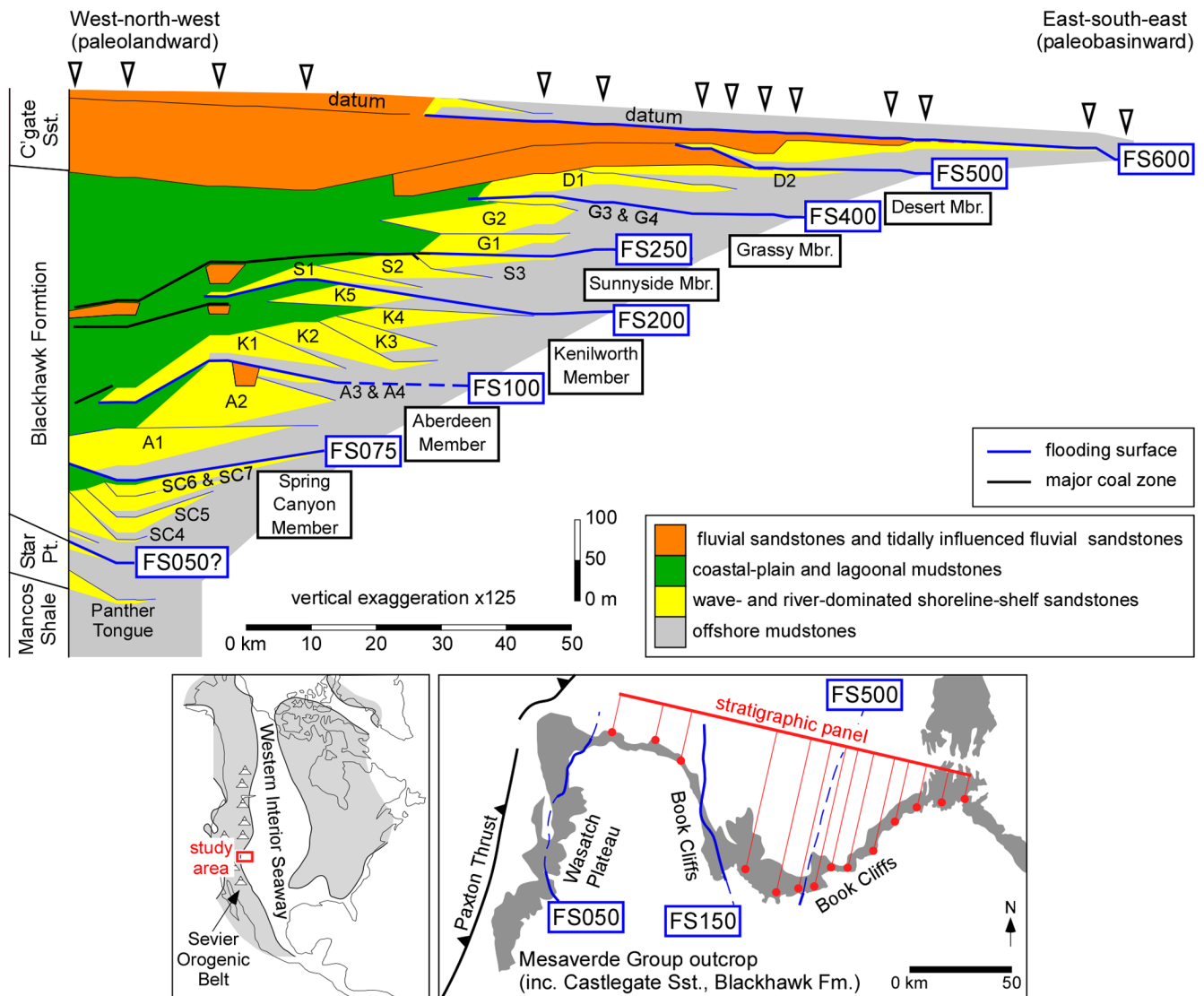


**FIGURE 1** Panel illustrating the stratal architecture of the Blackhawk Formation and related strata in the Book Cliffs outcrop belt (after Hampson, 2010; Hampson et al., 2014 and references therein). Regional flooding surfaces, members of the Blackhawk Formation, and the 22 shallow-marine sandstone tongues considered in our analysis (SC4-7, A1-4, K1-5, S1-3, G1-4, D1-2) are labelled. Datum surfaces are assigned the depositional dip of an east-southeastward-dipping coastal plain or shelf profile. The panel is located in the inset map (bottom right), which also shows palaeoshoreline positions for sandstone tongues directly below FS050, FS150 (K4 sandstone tongue) and FS500 (after Hampson, 2010; Hampson et al., 2011), and the inset palaeogeographical reconstruction of the Western Interior Seaway (bottom left; after Kauffman & Caldwell, 1993).

subaqueous clinoform (Hampson, 2010). The deposits were part of an extensive north-south trending linear coastline built into a broad, north-south trending basin, the Cretaceous Western Interior Seaway of North America, which developed in response to thrusting and subduction along its western margin (Li & Aschoff, 2022; Liu et al., 2014).

The Blackhawk Formation is comprised of six members (Figure 1): the Spring Canyon Member, the Aberdeen Member, the Kenilworth Member, the Sunnyside Member, the Grassy Member, and the Desert Member. These consist of continental to shallow-marine deposits, with their

offshore equivalent represented by the Mancos Shale. The continental deposits consist of sandstone-poor coal-bearing coastal plain deposits with some interspersed fluvial channel-belt sandstones (e.g. Hampson et al., 2012). The shallow-marine deposits were deposited by a prograding wave-dominated deltaic shoreline building out into waters 15–50 m deep. A large part of their offshore equivalent mudstone deposits comprises a mud belt defining a subaqueous clinoform with topsets located at a depth of about 50–80 m (Hampson, 2010). Blackhawk palaeoshorelines were linear to gently curved and oriented between N-S and NNE-SSW (Figure 1). The shorelines

were fed by multiple small rivers, as indicated by stratigraphic architectures (e.g. Hampson et al., 2011) and drainage reconstruction using detrital zircon U-Pb data (Pettit et al., 2019), with sand reworked by longshore currents (e.g. Hampson, 2010). The Blackhawk Formation is overlain by the Castlegate Sandstone, which consists of amalgamated sandstones deposited by braided rivers (e.g. Miall, 1994; Van Wagoner, 1995). Twenty-two discrete sandstone tongues each representing a progradational shoreface package, 13 ammonite biozones (Cobban et al., 2006; Gill & Hail, 1975), nine major regional flooding surfaces (Hampson, 2010), and two sub-regional erosional surfaces (Hampson et al., 2014) have been mapped out within the Blackhawk Formation/Mancos Shale succession. The shoreline-clinoform trajectory recorded by the near-shore sandstone belts exhibits a saw tooth pattern superimposed on the overall normal-regressive trend expressed by the system (Hampson, 2010).

The relationship between the ammonite biozones, regional flooding surfaces, and the Blackhawk Formation members mapped out in the Book Cliffs and Wasatch Plateau is presented in Table 1. The erosional base of the Castlegate Sandstone (Figure 1) is diachronous (e.g. Pattison, 2019), and the top of the underlying Blackhawk

Formation has been dated at ca. 76–80Ma in different locations using detrital zircon U-Pb chronology (Pettit et al., 2019). These dates are consistent with the published ages of ammonite biozones (Table 1).

### 3 | METHOD

#### 3.1 | Hypothesis

The Blackhawk Formation was deposited as part of a nearly linear coastline that grew by aggradation and progradation (Figure 1; e.g. Hampson, 2010; Hampson et al., 2011, 2014). We have limited ourselves only to estimate the time represented by shoreline progradation driven by deltaic sediment input since (i) shoreline progradation trajectories are well documented in the literature (Helland-Hansen & Hampson, 2009); (ii) they are documented to maintain high stratigraphic completeness (Mahon et al., 2015); (iii) there exists a suitable model to compare progradation rates with trajectories (Aadland & Helland-Hansen, 2019). The obvious consequences of limiting our window of observation to the shoreline trajectories are that we do not capture time associated with fluvial and offshore sedimentation

**TABLE 1** Relationship between the ammonite biozones, regional flooding surfaces, and members of the Blackhawk Formation

Formation	Member	FS	Ammonite biozone	Basal age (Ma)
Blackhawk Formation	Castlegate Sandstone/ Desert Member	FS600	Baculites gilberti	
			Baculites sp. (smooth)	
	Desert Member	FS500	Baculites asperiformis	
	Grassy Member	FS400	Baculites maclearni	
			Baculites obtusus	80.58 ± 0.55
	Sunnyside Member	FS250	Baculites sp. (weak flank ribs)	
	Kenilworth Member	FS200	Baculites sp. (smooth)	
Aberdeen Member	FS100	Scaphites hippocrepis III		
Spring Canyon Member	FS075	Scaphites hippocrepis II	81.86 ± 0.36	
		FS050	Scaphites hippocrepis I	

*Note:* The FS column represents regional flooding surfaces identified within the formation (Figure 1). Ammonite biozones from Gill and Hail (1975) and Cobban et al. (2006), and basal ages from radiometric datings in Cobban et al. (2006). The stratigraphic interval between FS050 and FS500 is analysed in this paper.

and that the time represented by elements of the shoreline trajectory succession lost through later erosion of shoreface deposits will be missing from our estimates. According to Aadland et al. (2018), the stratigraphic completeness of two-dimensional dip-oriented stratigraphic cross-sections through these deposits should be high unless erosion of parts of the formation took place subsequent to its deposition or sediment deposition has occurred outside our defined window of observation.

Aadland et al. (2018) predict that depositional elements that only grow in one direction will be free of scaling-induced timescale dependence. We argue that even though shoreline trajectories have both a progradational and aggradational component, a growth-in-one-direction approach in the case of linear prograding shorelines can be justified. The argument is as follows (see Table 2 for summary of parameters and notations used in our analysis):

- (i) It is observed that there is a limited thickness variation in the shoreface facies-belts of the Blackhawk Formation as reflected in the height of shoreline clinoforms being from five meters to a few tens of meters (Helland-Hansen & Hampson, 2009; Patruno & Helland-Hansen, 2018).
- (ii) We assume that the thickness of shoreface facies belts reflect the thickness of the prograding deltaic system.
- (iii) We argue that deltaic shoreline progradation is driven by sediment supply, and not by sea-level falls and forced regression. This is in accordance with the depositional models of Kamola and Van Wagoner (1995), Hampson (2010) and Pattison (2020).
- (iv) We highlight that if both the clinoform height ( $h$ ) and the width ( $w$ ) of the prograding deltaic system are constant, then the volume of the near-shore sandstone belt is only dependent on the length ( $l$ ) of progradation (Figure 2a).

Repeated deltaic shoreline progradation episodes followed by significant transgressions drive shoreline progradation trajectories to form an intricate pattern of multiple overlapping surfaces in three-dimensional space (Figure 2b). Asserting then that the volume of the shoreface facies-belt is dependent on only one direction of growth, we predict that the cumulative progradation distance represented by such deposits is free of scaling-induced timescale dependence.

We argue that there is a relation between modern deltaic progradation rates and the cumulative time captured by deltaic shoreline progradation of ancient shallow-marine sandstone bodies. Explicitly, our hypothesis is that duration of delta progradation quantified by considering the sum of the prograded areas (see Figure 1) in combination with progradation rates derived from modern systems, using the progradation rate model of Aadland and Helland-Hansen (2019), should represent a significantly larger portion of the biostratigraphically constrained time than what can be retrieved from empirically derived sedimentation rates from modern-day aggradation and progradation rates.

Below we consider the validity of assuming constant  $h$  and  $w$  for the shoreline clinoforms of the Blackhawk Formation. Published correlation panels, palaeogeographical reconstructions and isopach maps (e.g. Hampson, 2010) indicate that there is relatively little variability in the continuity, dip extent, and thickness of Blackhawk Formation shallow-marine strata along depositional strike (NNE-SSW) between outcrop belts along the southern (Books Cliffs, Wasatch Plateau; e.g. palaeoshoreline trends shown in Figure 1) and northern margins of the Uinta Basin. For different shallow-marine sandstone tongues, this corresponds to a depositional strike extent along the palaeoshoreline of between 50 km (SC4-7, A1-4, K1-5 tongues; Figure 1) and 200 km (S1-3, G1-4, D1-2 tongues; Figure 1),

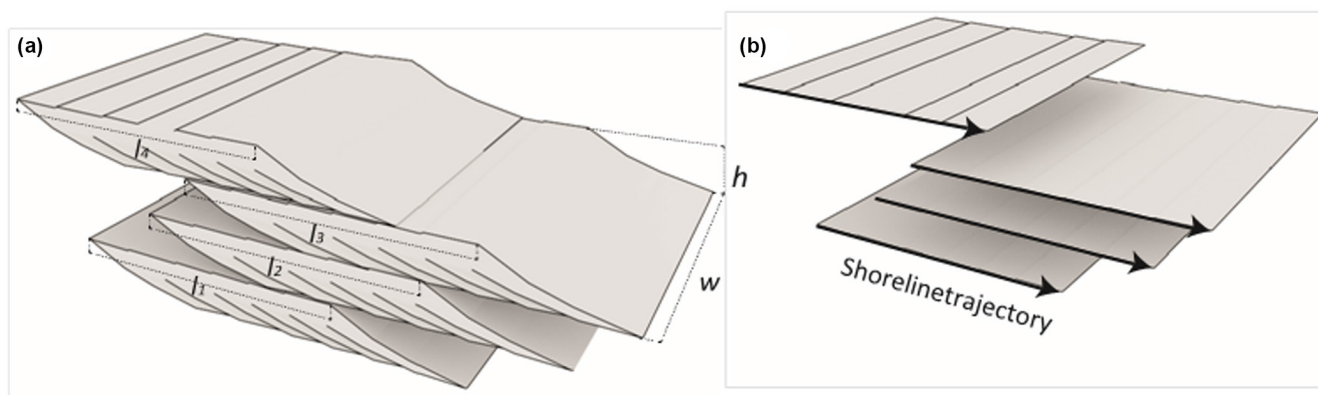


**FIGURE 2** (a) Stacked set of four progradational clinoform packages. Note that if the height  $h$  and width  $w$  are constant and known, then the clinoform package volume can be estimated by only knowing the length prograded  $l$ . (b) Three-dimensional representation of the cumulative area prograded in (a).

TABLE 2 List of parameters

Notation	Definition	Dimensions
$A_{catch}$	Catchment area	$L^2$
$A_{pro}$	Area of delta progradation (i.e. the product of $l$ and $w$ )	$L^2$
$B$	Factor quantifying sediment trapping, glacial, lithological, and anthropogenic effects in the calculation of $Q_s$ using BQART model of Syvitski and Milliman (2007)	–
$c_{on}$	Proportion of sand transported by the fluvial system that is captured and preserved in the onshore sediment repository in the model of Aadland and Helland-Hansen (2019)	–
$c_{sh}$	Proportion of sand transported by the fluvial system that is captured and preserved in shallow-marine sediment repository in the model of Aadland and Helland-Hansen (2019)	–
$c_{of}$	Proportion of sand transported by the fluvial system that is captured and preserved in offshore sediment repository in the model of Aadland and Helland-Hansen (2019)	–
$f_{ro}$	Runoff per unit area of catchment	$LT^{-1}$
$h$	Deltaic clinoform height	$L$
$l$	Length of delta progradation	$L$
$L_{pro}$	Cumulative length of progradation of shoreline segment of width $W_{catch}$	$L$
$L_{catch}$	Drainage length	$L$
$M_{of}$	Offshore sediment repository in the model of Aadland and Helland-Hansen (2019)	$L^3$
$M_{on}$	Onshore sediment repository in the model of Aadland and Helland-Hansen (2019)	$L^3$
$M_{sh}$	Shallow-marine repository in the model of Aadland and Helland-Hansen (2019)	$L^3$
$Q_{as}$	Along-shore sediment flux in the model of Aadland and Helland-Hansen (2019)	$L^3T^{-1}$
$Q_{fl}$	Fluvial sediment flux in the model of Aadland and Helland-Hansen (2019)	$L^3T^{-1}$
$Q_{os}$	Offshore sediment flux in the model of Aadland and Helland-Hansen (2019)	$L^3T^{-1}$
$Q_s$	Suspended sediment load	$MT^{-1}$
$Q_w$	Catchment water discharge	$L^3T^{-1}$
$r_{pro}$	Average areal progradation rate for analogous modern delta systems	$L^2T^{-1}$
$\bar{r}_{pro}$	Average areal progradation rate at the fluvial entry point for analogous modern deltaic systems, using the model of Aadland and Helland-Hansen (2019)	$L^2T^{-1}$
$r_{ref}$	Areal progradation rate averaged over the period $t_{ref}$	$L^2T^{-1}$
$R$	Maximum catchment relief	$L$
$t_{est}$	Time needed to prograde the area $A_{pro}$ given areal progradation rate $r_{pro}$	$T$
$t_{ref}$	Independent reference estimate of time represented by strata of interest	$T$
$T$	Mean catchment temperature	$\Theta$
$w$	Width of delta system	$L$
$W_{catch}$	Outlet spacing of catchments	$L$
$\omega$	Empirical constant for calculation of $Q_s$ using BQART model of Syvitski and Milliman (2007) (0.0006 for $Q_s$ calculated in units of $MT/yr$ )	$MT^{-0.69} L^{-2.93} \Theta^{-1}$

depending on subsurface well data constraints within the Uinta Basin and outcrop data constraints along its northern margin. Therefore, a 2D cross-section aligned WNW-ESE, perpendicular to the regional palaeoshoreline trend (Figure 1), is a reasonable, first-order simplification of 3D stratigraphic architecture in the Blackhawk Formation (cf. Hampson et al., 2014). We use the estimated along-strike spacing of drainage outlets at the Sevier Orogen front,  $W_{catch}$ , as a value of  $w$  (Section 3.5), which assumes that progradation is spatially averaged along the corresponding regional palaeoshoreline extent. Local spatial

variations in deltaic shoreline progradation, marked by subtle clinoform downlap and onlap relationships, are documented within sandstone tongues and attributed to the switching of wave-dominated delta lobes (e.g. Charvin et al., 2010; Hampson & Storms, 2003). By spatially averaging such variations in  $w$ , we temporally average the effects of delta lobe switching and thus consider sandstone tongues as the smallest stratigraphic units in our analysis. Therefore, non-depositional and erosional surfaces within sandstone tongues do not contribute to the “missing time” in our analysis. In contrast, regionally extensive surfaces

associated with transgression and/or basinward sediment bypass at the top of sandstone tongues do contribute to this “missing time”.

Palaeoshorelines in the Blackhawk Formation sandstone tongues have low rugosity over mapped depositional strike extents of 50–200 km, giving values of  $w$  that are 1.0–1.1 times greater than those of corresponding linear palaeoshorelines. Thus,  $w$  may be over-estimated by up to 10% by our assumption of a linear shoreline (cf. Figure 2). In contrast, the older Panther Tongue (Figure 1), which is not included in our study, contains a large SSE-to-SE-oriented delta that protruded from a gently curved N-S-trending palaeoshoreline (fig. 11B of Hampson et al., 2011), resulting in a value of  $w$  that is 1.7 times greater than that of a linear palaeoshoreline over a depositional strike extent of 90 km.

Sandstone thickness is a proxy for shoreline cliniform height,  $h$ , and varies little over the progradational extent of the palaeoshoreline in each sandstone tongue (e.g. Kamola & Van Wagoner, 1995; Hampson & Storms, 2003; Charvin et al., 2010), although sandstones thin down-dip of the most regressive palaeoshoreline position (cf. Figure 2a). Maximum sandstone thickness varies between the studied sandstone tongues, from 6 m (SC6 tongue) to 41 m (K5 tongue) (fig. 15C of Hampson, 2010) with a mean value of 23 m and a standard deviation of 10 m. Thus, we anticipate that values of  $h$  will show similar variations between the studied sandstone tongues, although there is likely to be less uncertainty in the mean value of  $h$  (ca. 10%). We use the method of Aadland and Helland-Hansen (2019), which is two-dimensional and characterises the changes in sandstone tongue area during progradation (the product of  $l$  and  $w$  in Figure 2). Consequently, unit thickness ( $h$  in Figure 2) is not accounted for in our analysis.

### 3.2 | Test of hypothesis

To test our hypothesis, we need three estimates:

- (i) An independent reference estimate of the time  $t_{ref}$  represented by the rocks (Section 3.3).
- (ii) An estimate of the area  $A_{pro}$  (the product of  $l$  and  $w$ ; Figure 2a) is represented by the cumulative sedimentation-driven deltaic shoreline progradation that has occurred during the deposition of the rocks. This can be estimated by steps I, II, III and IV of Table 3.
- (iii) An estimate of the average modern areal progradation rate  $r_{pro}$  (i.e. area generated by progradation per unit time) characterising deltaic systems with similar catchment and climate properties. This can be estimated by steps I, V, VI and VII of Table 3.

TABLE 3 Steps to produce time estimates

I.	Estimate catchment area using channel-belt thickness and estimated paleochannel depth (Section 3.4)
II.	Estimate outlet spacing using results from step I (Section 3.5). We treat outlet spacing as the width of the depositional system
III.	Estimate the cumulative distance covered by all shoreline transits recorded by shallow-marine sandstone bodies in a two-dimensional dip-oriented stratigraphic cross-section (Section 3.6)
IV.	Estimate the cumulative area covered by all shoreline transits using steps II and III (Section 3.6)
V.	Estimate water discharge ( $Q_w$ ) using catchment area and wetness estimated for the climate (Section 3.7)
VI.	Estimate suspended sediment load ( $Q_s$ ) using the BQART model (Syvitski & Milliman, 2007). Input is the results from steps I and V and additional catchment parameters (Section 3.8)
VII.	Estimate the progradation rate using $Q_w/Q_s$ . Input is the results from steps V and VI (Section 3.9)

With these three estimates, it is possible to estimate the time needed to account for the recorded deltaic shoreline progradation. The following equation expresses our hypothesis:

$$\frac{t_{est}}{t_{ref}} = \frac{A_{pro}}{(t_{ref} r_{pro})} = \frac{r_{ref}}{r_{pro}}, \quad (1)$$

where  $r_{ref}$  represents the average areal progradation rate of the deposit (in  $\text{km}^2/\text{yr}$ ) averaged over an averaging period  $t_{ref}$  (in yr), and  $t_{est}$  is the time (in yr) needed to prograde the area  $A_{pro}$  (in  $\text{km}^2$ ) given an areal progradation rate  $r_{pro}$  (in  $\text{km}^2/\text{yr}$ ) (cf. Aadland & Helland-Hansen, 2019).

### 3.3 | Determining $t_{ref}$

Eight ammonite biozones have been identified within the Blackhawk Formation. Absolute ages are only available for two of these, and these two ages have an uncertainty of plus-minus half a million years (Table 1). This uncertainty is significant, considering that the two ages are separated by only 1.3 million years. Hampson et al. (2014) present an age model of the deposits that quantifies the duration represented by each of its six members (Table 4). This age model is based on regional mapping of the ammonite-bearing flooding surfaces that bound the members, calibrated to the average duration of each ammonite biozone within periods constrained by radiometric dates (Krystinik & DeJarnett, 1995). The age model indicates that the total time represented by the Blackhawk Formation is 3.1 My. More recently, detrital

**TABLE 4** Ages represented by members of the Blackhawk Formation

Member	Age model from Hampson et al. (2014)	Absolute datings
Desert Member	0.5 My	
Grassy Member	0.8 My	1.3 ± 0.9 My
Sunnyside Member	0.4 My	
Kenilworth Member	0.3 My	
Aberdeen Member	0.5 My	
Spring Canyon Member	0.6 My	

zircon U-Pb chronology has been used to date the diachronous contact between the Blackhawk Formation and overlying Castlegate Sandstone at ca. 76–80 Ma (Pettit et al., 2019). Although these dates are consistent with the radiometric dates of ammonite biozones (Table 1), both sources of dates imply that the duration of each member of the Blackhawk Formation (Table 4) may be increased or decreased by a factor of ca. 2. We sum the duration of each member in the age model of Hampson et al. (2014) to estimate  $t_{ref}$  and halve and double this value to represent uncertainty. The resulting minimum, median and maximum values of  $t_{ref}$  are 1.6, 3.1 and 6.2 My.

### 3.4 | Estimating catchment area

Whilst the sedimentary deposits themselves are largely unaffected by post-depositional modification, the sediment source area and alluvial hinterland have been significantly altered by structural deformation and erosion (e.g. DeCelles & Coogan, 2006; Hampson et al., 2014; Lawton, 1986; Pettit et al., 2019) and must be constrained by proxies. Hampson et al. (2014) used channel bar thicknesses to estimate the mean bank full paleochannel depth to be 6–9 m for the Blackhawk Formation, and used this estimate in conjunction with the scaling relationships in Blum et al. (2013) (their fig. 5) to infer that the Blackhawk Formation rivers probably drained a catchment area,  $A_{catch}$ , of  $1 \times 10^4$ – $5 \times 10^4$  km<sup>2</sup>, which we simplify to  $3 \pm 2 \times 10^4$  km<sup>2</sup>.

Although the scaling relationship described above to estimate  $A_{catch}$  fits well with data from the late Pleistocene to modern river systems ( $R^2 = 0.745$ ; Blum et al., 2013), it does not provide a perfect fit. A wider range of values for  $A_{catch}$ , from  $2 \times 10^3$  km<sup>2</sup> to  $5 \times 10^5$  km<sup>2</sup>, is given by geomorphic regional curves for palaeochannels of similar depth (5–9 m), paleolatitude (40°N) and humid, subtropical paleoclimate along the western margin of the Western Interior Seaway (Ferron Sandstone in Table 2 of Davidson & North, 2009). We use the smaller range of values for  $A_{catch}$  ( $1 \times 10^4$ – $5 \times 10^4$  km<sup>2</sup>) outlined in the preceding paragraph in our analysis, rather than the larger range of  $A_{catch}$

values, which exceeds two orders of magnitude. The latter range would include catchments that are sufficiently large to extend into the Cretaceous Cordilleran magmatic arc, which is inconsistent with available U–Pb geochronological and petrographic data (Dickinson & Gehrels, 2010; Lawton & Bradford, 2011).

### 3.5 | Estimating outlet spacing

Outlet spacing is an essential parameter in source-to-sink analysis, as it quantifies the number of sediment source areas that terminate in the depositional sink. Palaeoshoreline trends in sandstone tongues that underlie the Blackhawk Formation in the Wasatch Plateau outcrop belt (e.g. palaeoshoreline position below FS050 in Figure 1) consistently define a broad, eastward-facing concave geometry (e.g. Edwards et al., 2005; Hampson et al., 2011). This concave geometry has been speculatively attributed to long-lived sediment routing through outlets at the northern and southern tips of the syn-depositional Paxton Thrust (Figure 1), which lay ca. 30 km west of the Wasatch Plateau outcrop belt (Edwards et al., 2005) and ca. 50 km east of sediment sources at the front of the Sevier Orogen (Hampson et al., 2014). These inferred drainage outlets have a spacing of ca. 90–110 km. Small deltaic protrusions are superimposed on the concave palaeoshoreline trends (Hampson et al., 2011), implying that there may have been additional outlets and thus smaller outlet spacing. The interpretation outlined above is supported by drainage reconstruction for the Blackhawk Formation using detrital zircon U-Pb data (Pettit et al., 2019); four spatially distinct parent rivers are interpreted to have supplied the Blackhawk Formation in the Wasatch Plateau outcrop belt, implying a mean outlet spacing of ca. 40 km.

An alternative approach is to estimate outlet spacing using geometrical considerations and scaling relationships, although these are associated with significant uncertainties. If we assume that the catchments feeding sediments to the coastline were equally spaced and sourced from a linear mountain belt, we can use the scaling relationship of Castellort and Simpson (2006) to estimate catchment spacing. Castellort and Simpson (2006)

explored a numerical model of drainage network growth in mountain ranges, and their analysis suggests that the outlet spacing of such a system is as follows:

$$W_{catch} = 0.5L_{catch}, \quad (2)$$

where  $W_{catch}$  is the outlet spacing, and  $L_{catch}$  is the drainage length. Hampson et al. (2014) used data from Hovius (1996) to present the following variation of Hack's law for evaluating the drainage length of the Blackhawk Formation rivers:

$$L_{catch} = 1.48A_{catch}^{0.49}, \quad (3)$$

This formula indicates that the value of  $L_{catch}$  for the Blackhawk Formation rivers was between 140 and 300 km (for  $A_{catch}$  of  $1 \times 10^4$  and  $5 \times 10^4$  km<sup>2</sup>, respectively), with a median of 230 km (for  $A_{catch}$  of  $3 \times 10^4$  km<sup>2</sup>). By combining Equation (3) with Equation (2), we arrive at values of  $W_{catch}$  between 68 and 150 km (for  $A_{catch}$  of  $1 \times 10^4$  and  $5 \times 10^4$  km<sup>2</sup>, respectively), with a median of 120 km (for  $A_{catch}$  of  $3 \times 10^4$  km<sup>2</sup>). Using the broader range of values for  $A_{catch}$  given by geomorphic regional curves in Equations (2) and (3), outlet spacing lies between 31 and 460 km. These estimates of outlet spacing are consistent with the observational constraints from the Wasatch Plateau and Book Cliffs outcrop belts.

### 3.6 | Estimating area of deltaic shoreline progradation

As outlined earlier (Section 3.1), we argue that a two-dimensional dip-oriented stratigraphic cross-section of

the Blackhawk Formation is reasonably representative of the three-dimensional configuration of these strata for 200 km along depositional strike. This justifies treating two-dimensional cross-sectional stratigraphic data as a 2.5-dimensional representation of the Blackhawk Formation. Thus, the shoreline progradation area of the system is entirely described by outlet spacing and such two-dimensional cross-sections.

We are interested in estimates of cumulative deltaic shoreline progradation distance driven by sedimentation and quantify this by considering the shoreline progradation distance recorded in the shallow-marine sandstone bodies. Explicitly, we measure the horizontal component of the coastal-plain and lagoonal mudstones to wave- and river-dominated shoreline-shelf sandstone transitions in the correlation panel of Hampson et al. (2014), at the resolution of individual shallow-marine sandstone tongues in each member of the Blackhawk Formation (i.e. 22 sandstone tongues in Figure 1). These measurements are summarised in Table 5.

The Blackhawk Formation deposits were part of a north-south trending linear coastline sourced from multiple adjacent catchments; consequently, it is not trivial to relate shoreline changes at one location to one specific source area. We deal with this by segmenting the linear coastline according to the outlet spacing estimated in the preceding section (Figure 3).

The progradational area associated with each catchment is then given by:

$$A_{pro} = L_{pro}W_{catch}, \quad (4)$$

where  $L_{pro}$  is the cumulative distance prograded. We use the range of values of  $W_{catch}$  derived from  $A_{catch}$  estimates

Member	$L_{pro}$ (km)	$A_{pro}$ (km <sup>2</sup> )	$r_{ref}$ (km <sup>2</sup> /yr)
Desert (D1 + D2)	45	2700, 5200, 7400	0.003, 0.01, 0.03
Grassy (G1 + G2 + G3 + G4)	18	1100, 2100, 2900	0.0007, 0.003, 0.007
Sunnyside (S1 + S2 + S3)	66	4000, 7600, 11,000	0.005, 0.02, 0.05
Kenilworth (K1 + K2 + K3 + K4 + K5)	58	3500, 6700, 9500	0.006, 0.02, 0.06
Aberdeen (A1 + A2 + A3 + A4)	48	2900, 5600, 7800	0.003, 0.01, 0.03
Spring Canyon (SC4 + SC5 + SC6 + SC7)	25	1500, 2900, 4100	0.001, 0.005, 0.01
Combined total	260	16,000, 30,000, 42,000	0.003, 0.01, 0.03

Note: The sandstone tongues in each member (Figure 1) are listed in parentheses. Minimum, median and maximum estimates of progradational area,  $A_{pro}$ , and time-averaged areal progradation rate,  $r_{ref}$ , are given (see text for details).

TABLE 5 Cumulative distances of shoreline progradation,  $L_{pro}$ , recorded in Blackhawk Formation members (from fig. 15A of Hampson, 2010) and for the entire studied interval of the Blackhawk Formation

applied to Equations (2) and (3) (i.e. 68–150 km with a median of 120 km; Section 3.5) and values of  $l_{pro}$  measured from the Book Cliffs outcrop belt (from fig. 15A of Hampson, 2010), with a range of  $\pm 10\%$  to account for the effect of palaeoshoreline rugosity (Section 3.1) in our estimates of  $A_{pro}$  (Table 5). Time-averaged areal progradation rate,  $r_{ref}$  is estimated from the resulting values of  $A_{pro}$  and the age model of Hampson et al. (2014) (Table 4), but with the duration of Blackhawk Formation members increased or decreased by a factor of ca. 2 to account for uncertainty in this model (Table 5). Estimates of  $r_{ref}$  range over two orders of magnitude, from  $0.0007 \text{ km}^2/\text{yr}$  (minimum estimate, Grassy Member) to  $0.06 \text{ km}^2/\text{yr}$  (maximum estimate, Kenilworth Member). Over the 22 sandstone tongues in the studied interval of the Blackhawk Formation, the minimum, median and maximum estimates of  $r_{ref}$  are 0.003, 0.01 and  $0.03 \text{ km}^2/\text{yr}$  (Table 5).

### 3.7 | Estimating water discharge

We can estimate the catchment water discharge from

$$Q_w = f_{ro} A_{catch}, \quad (5)$$

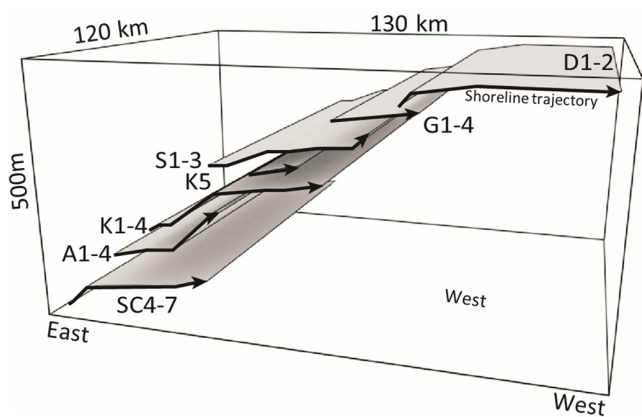


**FIGURE 3** The cumulative deltaic shoreline progradation recorded by shallow-marine sandstone tongues of the Blackhawk Formation (Figure 1, Table 5) plotted in three-dimensional space. The model is drawn assuming a linear coastline and an outlet spacing of 120 km.

**TABLE 6** Summary of the parameters used to estimate the suspended sediment load with the BQART model (Syvitski & Milliman, 2007)

Parameter	Value
$\omega$	0.0006 (for units of MT/yr)
$B$	1
$Q_w$	2.5 (min.), 15 (median), 37.5 (max.) $\text{km}^3/\text{yr}$ (Section 3.7)
$A_{catch}$	$30,000 \pm 20,000 \text{ km}^2$ (Section 3.4)
$R$	$2 \pm 1 \text{ km}$
$T$	$15 \pm 5^\circ\text{C}$

where  $Q_w$  is the catchment water discharge, and  $f_{ro}$  is the catchment runoff. Catchment runoff is a climate parameter and must be estimated by using climate proxies. The abundance of coal in Blackhawk Formation coastal-plain deposits suggests that the catchment climate was warm and humid (Kauffman & Caldwell, 1993), whilst a more detailed investigation of the coal flora supports this by indicating a warm-temperate to subtropical seasonal climate (Parker, 1976). In approximately coeval (ca. 76 Ma), coal-bearing deposits in the Kaiparowits Formation of southern Utah, mean annual temperature and mean annual precipitation are estimated to have been  $20^\circ\text{C}$  and 1800 mm, respectively, based on palaeofloral analysis of leaf morphology (Miller et al., 2013). A humid climate suggests that  $f_{ro}$  was about  $500 \pm 250 \text{ mm}/\text{yr}$  per unit area ( $\text{km}^2$ ) (Milliman & Farnsworth, 2013). Using Equation (5), we then estimate minimum, median and maximum values of  $Q_w$  to be 2.5, 15 and  $37.5 \text{ km}^3/\text{yr}$ , respectively, for  $A_{catch}$  values of  $1 \times 10^4$ ,  $3 \times 10^4$  and  $5 \times 10^4 \text{ km}^2$ , respectively (Section 3.5).

### 3.8 | Estimating suspended sediment load

We use the BQART model of Syvitski and Milliman (2007) to estimate the suspended sediment load,  $Q_s$ . It has the following form:

$$Q_s = \omega B Q_w^{0.31} A_{catch}^{0.5} R T, \quad (6)$$

where  $\omega$  is a constant,  $B$  is a factor that quantifies sediment trapping, glacial, lithological and anthropogenic effects,  $R$  is maximum relief in the catchment, and  $T$  is the mean catchment temperature. For further explanation and justification of the individual parameters, we refer to Syvitski and Milliman (2007). Structural reconstruction made by DeCelles and Coogan (2006) implies that the relief of the Blackhawk Formation catchment was in the range of 1000–3000 m, whilst the paleoclimate was warm to temperate (Kauffman & Caldwell, 1993; Parker, 1976). We estimate  $Q_s$  to range between 1 and 25 MT/yr, with a median of 7 MT/yr, using the BQART model with these parameters (Table 6). These estimates are based on the assumption

that the constituent parameters and the total sediment load were constant during the time span of deposition of the Blackhawk Formation.

### 3.9 | Estimating progradation rates

We use the progradation rate model presented in Aadland and Helland-Hansen (2019) to estimate the average progradation rate. They analysed Landsat 4, 5, 7 and 8 derived satellite images acquired in the period 1984 to 2015 to create a compilation of modern deltaic areal progradation rates. These rates were compared with catchment and climate parameters compiled in Milliman and Farnsworth (2013). This analysis produced a statistical model of the progradation rates that only take fluvial water discharge and suspended sediment load as input. The model has the following form:

$$\bar{r}_{pro} = 10^{-2.3} Q_w^{0.59} Q_s^{0.34}, \quad (7)$$

where  $\bar{r}_{pro}$  is the predicted average areal progradation rate [ $\text{km}^2/\text{yr}$ ] at the deltaic system's fluvial entry point,  $Q_w$  is the water discharge of the associated fluvial system in  $\text{km}^3/\text{yr}$ , and  $Q_s$  is the total suspended sediment delivered by the fluvial system in  $\text{MT}/\text{yr}$  (eq. 18 in Aadland & Helland-Hansen, 2019). Using the range of values of  $Q_w$  and  $Q_s$  estimated previously (Section 3.8), we use the model to estimate minimum, median and maximum values of  $\bar{r}_{pro}$  of 0.008, 0.05 and  $0.1 \text{ km}^2/\text{yr}$ .

## 4 | RESULT

We use the method outlined above to calculate the proportion of available time accounted for by progradation,  $\frac{t_{est}}{t_{ref}}$ , using Equation (1). We use minimum, median and maximum estimates of  $r_{ref}$  of 0.003, 0.01 and  $0.03 \text{ km}^2/\text{yr}$  (Section 3.6; Table 5), and minimum, median and maximum estimates of  $\bar{r}_{pro}$  of 0.008, 0.05 and  $0.1 \text{ km}^2/\text{yr}$  (Section 3.9) in our calculation. These estimates are based on values of  $L_{pro}$ ,  $A_{catch}$ ,  $B$ ,  $R$ ,  $T$ ,  $f_{ro}$  and  $t_{ref}$  outlined previously (Sections 3.1–3.9) and summarised in Table 7. The resulting minimum, median and maximum estimates of

$\frac{t_{est}}{t_{ref}} \left( = \frac{r_{ref}}{\bar{r}_{pro}} \right)$  are, respectively, 0.02, 0.2 and 3. These estimates span two orders of magnitude, reflecting the propagation of uncertainty in each contributing parameter (Table 7). The median value indicates that we can readily account for 20% of the time available via delta progradation, whilst the minimum-to-maximum range implies that this percentage could be an order of magnitude lower or higher. The estimated value of  $\frac{t_{est}}{t_{ref}}$  is increased above its

TABLE 7 Summary of the parameters and their minimum, median and maximum values used to estimate the proportion of available time accounted for by progradation ( $\frac{t_{est}}{t_{ref}}$ ; Equation 1)

Parameter (units)	Minimum	Median	Maximum
$L_{pro}$ (km)	234	260	286
$A_{catch}$ ( $\text{km}^2$ )	10,000	30,000	50,000
$B$	1		
$R$ (km)	1	2	3
$T$ ( $^{\circ}\text{C}$ )	10	15	20
$\omega$	0.0006 (for units of $\text{MT}/\text{yr}$ )		
$f_{ro}$ ( $\text{km}/\text{yr}$ )	$250 \times 10^{-6}$	$500 \times 10^{-6}$	$750 \times 10^{-6}$
$t_{ref}$ (yr)	$1.6 \times 10^6$	$3.1 \times 10^6$	$6.2 \times 10^6$

median value of 0.2 by  $f_{ro}$ ,  $A_{catch}$ ,  $Q_w$ ,  $R$  and/or  $T$  above their median values, or by reducing  $t_{ref}$  below its median value (Table 7). More detailed quantification of uncertainty, such as Monte Carlo simulation (e.g. Brewer et al., 2020; Zhang et al., 2018), is complicated by the widely varying constraints offered by different methodological approaches (e.g. to estimate catchment area; Section 3.4) and lies beyond the scope of this paper. However, the simple approach adopted here is sufficient to provide a first-order assessment of time that is represented by delta progradation, and thus to test our hypothesis.

## 5 | DISCUSSION

### 5.1 | Is this a reasonable result?

This paper explores the viability of using an empirical model of progradation rates derived from modern deltaic coastlines to understand the duration of deposition of a stratigraphic succession that is constrained by biostratigraphy and radiometric datings to have occurred over a multi-million-year period. The progradation rate model was constructed from observations of depositional processes operating over 2 to 30 years; that is, about five to six orders of magnitude shorter than the duration over which the sedimentary rocks were deposited. Our analysis produced a median time estimate that is approximately five times shorter (20%) than the ca. 3.1 My reference time represented by the sedimentary rocks. This discrepancy is small when considering the timescale dependence of sedimentation rates, which indicates that both aggradation rates and progradation rates based on 2 to 30 years of observation should be about 300 to 1000 times faster than those characterising deposits that have accumulated over a 3 My period (Reineck, 1960; Sadler, 1981; Sadler & Jerolmack, 2015; Schindel, 1980). The estimated time represented by progradation can readily be increased

above 20% using higher-than-median values of catchment runoff ( $f_{ro}$ ), catchment area ( $A_{catch}$ ), catchment water discharge ( $Q_w$ ), catchment relief ( $R$ ), and/or mean catchment temperature ( $T$ ), or by using lower-than-median values of the independent reference time ( $t_{ref}$ ) (Table 7). The result demonstrates that the estimated duration of the Blackhawk Formation deltaic shoreline progradation represents a significant amount of time; consequently, we do not reject the hypothesis that the duration of delta progradation quantified by considering the sum of the prograded areas in combination with progradation rates derived from modern systems, using the progradation rate model of Aadland and Helland-Hansen (2019), should represent a significant portion of the biostratigraphically constrained time represented by the ancient deposits.

Since our result indicates that the empirical progradation rate model for modern deltaic coastlines of Aadland and Helland-Hansen (2019) can be reasonably used to estimate in 2D cross-section the duration of deposition for ancient shallow-marine strata, it follows that even simpler models can also be applied. For example, values of  $\bar{r}_{pro}$  taken from the model of Aadland and Helland-Hansen (2019) can be multiplied by  $t_{ref}$  to give 1D estimates of cumulative progradation lengths ( $L_{pro}$ ), provided that progradation at the fluvial entry point is representative of progradation of the whole deltaic shoreline. As for the 2D approach, this condition is likely to hold for wave-dominated deltas and contiguous strandplains with nearly linear shorelines, but not for rugose shorelines with significant along-strike variation in time-averaged progradation rate (e.g. in river-dominated deltas). Generally, our methodology also does not apply to ancient systems with highly variable thicknesses of shoreface facies belts (e.g. due to temporally changing wave regime), nor to systems in which progradation was largely driven by relative sea-level falls.

## 5.2 | Where is the missing time?

Our analysis demonstrates that deltaic shoreline progradation could account for ca. 20% (and potentially between 2% and 300%) of the available time of the Blackhawk Formation. By implication, the shoreline was not prograding ca. 80% of the time or evidence of such progradation has been removed by later erosion. This means that non-depositional and erosional discontinuities, including flooding surfaces and related transgressive deposits that bound each shallow-marine sandstone tongue, represent the missing time.

If the delivery of sandy material to the shoreline primarily drives deltaic progradation, it follows that the distribution of sandy deposits within the entire sediment

routing system may increase our understanding of where to attribute the missing time. We conceptualise this by considering the significant repositories of sandy material and the fluxes between them in a typical siliciclastic depositional system, as outlined in Aadland and Helland-Hansen (2019). This model is comprised of three different sediment repositories: Onshore ( $M_{on}$ ), shallow-marine ( $M_{sh}$ ), and offshore ( $M_{of}$ ). These are connected by three main sediment flux domains transporting sandy material; fluvial transport, alongshore transport, and offshore-directed transport. The ultimate source of sediment is represented by fluvial systems, which carry sediment downslope. This flux  $Q_{fl}$  affects the onshore, shallow-marine, and offshore repositories. Marine processes drive alongshore sediment transport that erodes and removes previously deposited sediment and introduces new sediment where the erosional products are laid down. This alongshore sediment flux  $Q_{as}$  primarily affects the shallow-marine deposits, whilst the offshore sediment flux  $Q_{os}$  is sourced from the shallow-marine deposits or direct fluvial feeding (e.g., hyperpycnites; Mulder et al., 2003) and terminated in the offshore environments. Mathematically, the system is described like this:

$$\frac{dM_{on}}{dt} = c_{on} \sum_{i=1}^n Q_{fl}(i), \quad (8)$$

$$\frac{dM_{sh}}{dt} = Q_{as} - Q_{os} + c_{sh} \sum_{i=1}^n Q_{fl}(i), \quad (9)$$

$$\frac{dM_{of}}{dt} = Q_{os} + c_{of} \sum_{i=1}^n Q_{fl}(i), \quad (10)$$

$$c_{on} + c_{sh} + c_{of} = 1, \quad (11)$$

where  $n$  is the number of fluvial systems terminating at the shoreline, and  $c_{on}$ ,  $c_{sh}$  and  $c_{of}$  are coefficients that quantify the ratio of the sandy material transported by the fluvial system that is captured and preserved within the onshore, shallow-marine, and offshore sediment repositories, respectively. Assuming then that the cumulative progradation rate of the deltaic shoreline is proportional to how much sandy material is delivered to and preserved in the shallow-marine environments, and that the deltaic clinof orm maintains a constant height ( $h$ ) during progradation, it follows that the following relationship describes it:

$$\sum_{i=1}^n r_{pro}(i) = c \frac{dM_{sh}}{dt}, \quad (12)$$

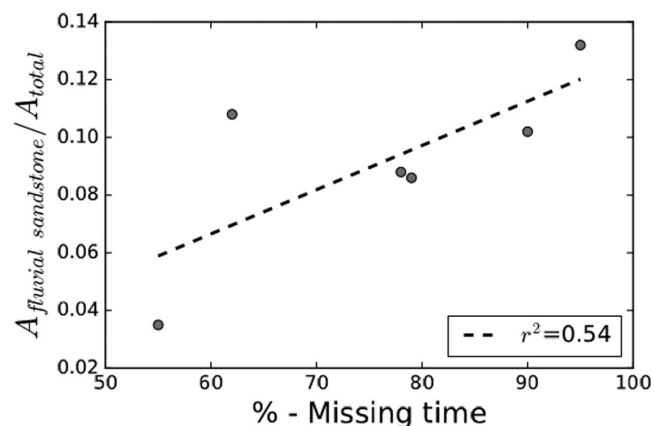


**FIGURE 4** Plot of the proportion of fluvial sandstones represented by the cross-sectional area (cf. Figure 1) of each member of the Blackhawk Formation against the median estimates of missing time, based on the age model of Hampson et al. (2014) (Table 4). Progradation distances are quantified in Hampson (2010), and areal progradation rates are estimated using the model of Aadland and Helland-Hansen (2019). The proportion of fluvial sandstones was calculated using the data presented in figs. 6 and 10 of Hampson et al. (2014).

where  $c$  is a proportionality constant. Non-depositional discontinuities could arise in this system if  $c_{sh}$  were decreased, that is, if less of the sandy material transported by the fluvial system was captured in the shallow-marine repository. Similarly, erosional discontinuities could form by an increase in  $Q_{os}$  or a negative  $Q_{as}$ ; that is, by an increase in offshore directed sediment transport, or if more sediment were removed by along-shore drift than was supplied. For a non-depositional discontinuity to represent the missing time in our analysis, it must occur over the entire coastline and thus bound a sandstone tongue. This could happen if the sediment supply is reduced to zero ( $Q_{fl} \approx 0$ ), if the sediment for some time was extracted from the fluvial sediment flux and deposited in the onshore repository before arriving at the shoreline ( $c_{on} \approx 1$ ) or if the sandy material delivered by the fluvial system bypassed the shoreface entirely ( $c_{sh} \approx 0$ ).

To investigate if the missing time in the shoreface domain could be attributed to the retention of sand on the alluvial plain (e.g. in levees, crevasse-splays and fluvial bars), we compare the missing time in each member of the Blackhawk Formation with the proportion of sand in the time-equivalent upstream alluvial succession. A weak positive correlation ( $r^2 = 0.5$ ) between the two properties indicates that some of the missing time might indeed be attributed to sediment retention on the alluvial plain (Figure 4) and that this retention may be represented by downstream shoreline-spanning non-depositional shoreface discontinuities or condensed sections (e.g. flooding surfaces in Figure 1).

## 6 | CONCLUSION

We assess the degree to which progradational shallow-marine strata provide a complete record of geological time by applying a recently developed geometrical model of time-averaged sedimentation and an empirical database of modern delta progradation rates to a well-documented ancient wave-dominated deltaic succession (Blackhawk Formation, Cretaceous Western Interior Seaway, USA). First, we assume that a two-dimensional dip-oriented cross-section through the Blackhawk Formation is a representative 2.5-dimensional model of the stratigraphy. We then use a catchment area estimate based on fluvial bar thicknesses and a calibrated form of Hack's law to estimate catchment length. This allowed us to make simple first-order estimates of the outlet spacing and hence the area of catchments delivering sediments to the linear coastline where the shoreface sandstone belt of the Blackhawk Formation was deposited. We assume that the coastline was fed by a series of adjacent drainage systems with similar catchment and climate properties. We then estimate the progradation rate for the deltaic shorelines based on empirical observations derived from modern deltaic coastlines with similar catchment properties as those inferred for the Blackhawk catchments. In this way, we can demonstrate that the amount of time needed to account for the cumulative progradation area recorded by the Blackhawk Formation rocks was about 20% ( $\pm$  approximately one order of magnitude) of the available chronostratigraphically constrained time. This discrepancy is small when considering the timescale dependence of sedimentation rates, which indicates that both aggradation rates and progradation rates based on 2-30 years of observation should be about 300-1000 times faster than those characterising deposits that have accumulated over a 3 My period, and the potential for time to be represented by flooding surfaces that punctuate the progradational shallow-marine strata. Furthermore, we demonstrate that the amount of missing time is weakly correlated with the proportion of sandstone in alluvial-to-coastal plain deposits, and argue that the lost time could be partly explained by the retention of sandy material on the floodplain. The method can be widely applied to other shallow-marine strata in order to estimate the time represented by deposition, particularly along coastlines that are well approximated by a 2.5-dimensional representation (e.g. wave-dominated and wave-influenced deltas with contiguous strandplains).

## ACKNOWLEDGEMENTS

We are grateful for the constructively critical reviews and editorial comments of Thomas Ashley, Liz Hajek,

Wonsuck Kim and an anonymous reviewer. This research was funded by ARCEX partners and the Research Council of Norway (grant number 228107).

## PEER REVIEW

The peer review history for this article is available at <https://publons.com/publon/10.1111/bre.12737>.

## DATA AVAILABILITY STATEMENT

The data that support the findings of this study are publicly available from the sources cited in the paper. No new data were created or analysed in this study.

## ORCID

Tore Aadland  <https://orcid.org/0000-0002-0861-4782>

Gary Hampson  <https://orcid.org/0000-0003-2047-8469>

William Helland-Hansen  <https://orcid.org/0000-0002-7529-1485>

## REFERENCES

- Aadland, T., & Helland-Hansen, W. (2019). Progradation rates measured at modern river outlets: A first-order constraint on the pace of deltaic deposition. *Journal of Geophysical Research: Earth Surface*, *124*, 347–364.
- Aadland, T., Sadler, P. M., & Helland-Hansen, W. (2018). Geometric interpretation of timescale dependent sedimentation rates. *Sedimentary Geology*, *371*, 32–40.
- Allen, P. A. (2017). *Sediment routing systems: The fate of sediment from source to sink*. Cambridge University Press.
- Balsley, J. K. (1980). *Cretaceous wave-dominated delta systems, Book Cliffs, east-central Utah*. American Association of Petroleum Geologists, Continuing Education Course Field Guide.
- Blum, M., Martin, J., Milliken, K., & Garvin, M. (2013). Paleovalley systems: Insights from quaternary analogs and experiments. *Earth-Science Reviews*, *116*, 128–169.
- Brewer, C. J., Hampson, G. J., Whittaker, A. C., Roberts, G. G., & Watkins, S. E. (2020). Comparison of methods to estimate sediment flux in ancient sediment routing systems. *Earth-Science Reviews*, *207*, 103217.
- Castelltort, S., & Simpson, G. (2006). Growing mountain ranges and quenched river networks. *Comptes Rendus Geoscience*, *338*, 1184–1193.
- Cattaneo, A., Correggiari, A., Langone, L., & Trincardi, F. (2003). The late-Holocene Gargano subaqueous delta, Adriatic shelf: Sediment pathways and supply fluctuations. *Marine Geology*, *193*, 61–91.
- Charvin, K., Hampson, G. J., Gallagher, K. L., & Labourdette, R. (2010). Intra-parasequence architecture of an interpreted asymmetrical wave-dominated delta. *Sedimentology*, *57*, 760–785.
- Cobban, W. A., Walaszczyk, I., Obradovich, J. D., & McKinney, K. C. (2006). *A USGS zonal table for the upper cretaceous middle Cenomanian—Maastrichtian of the western interior of the united states based on ammonites, inoceramids, and radiometric ages*. U.S. Geological Survey Open-File Report, 2006-1250.
- Davidson, S. K., & North, C. P. (2009). Geomorphological regional curves for prediction of drainage area and screening modern analogues for rivers in the rock record. *Journal of Sedimentary Research*, *79*, 773–792.
- DeCelles, P. G., & Coogan, J. C. (2006). Regional structure and kinematic history of the Sevier fold-and-thrust belt, Central Utah. *Geological Society of America Bulletin*, *118*, 841–864.
- Dickinson, W. R., & Gehrels, G. E. (2010). Insights into North American paleogeography and paleotectonics from U-Pb ages of detrital zircons in Mesozoic strata of the Colorado plateau, USA. *Geologische Rundschau*, *99*, 1247–1265.
- Edwards, C. M., Howell, J. A., & Flint, S. S. (2005). Depositional and stratigraphic architecture of the Santonian Emery Sandstone of the Mancos Shale: Implications for Late Cretaceous evolution of the Western Interior foreland basin of central Utah, USA. *Journal of Sedimentary Research*, *75*, 280–299.
- Gill, J. R., & Hail, W. J., Jr. (1975). *Stratigraphic sections across Upper Cretaceous Mancos Shale-Mesaverde Group boundary, eastern Utah and western Colorado*. U.S. Geological Survey, Oil and Gas Investigations Chart OC-68.
- Hajek, E. A., & Straub, K. M. (2017). Autogenic sedimentation in clastic stratigraphy. *Annual Review of Earth and Planetary Sciences*, *45*, 681–709.
- Hampson, G. J. (2010). Sediment dispersal and quantitative stratigraphic architecture across an ancient shelf. *Sedimentology*, *57*, 96–141.
- Hampson, G. J., Duller, R. A., Petter, A. L., Robinson, R. A., & Allen, P. A. (2014). Mass-balance constraints on stratigraphic interpretation of linked alluvial-coastal-shelfal deposits from source to sink: Example from cretaceous western interior basin, Utah and Colorado, USA. *Journal of Sedimentary Research*, *84*, 935–960.
- Hampson, G. J., Gani, M. R., Sahoo, H., Rittersbacher, A., Irfan, N., Ranson, A., Jewell, T. O., Gani, N. D. S., Howell, J. A., Buckley, S. J., & Bracken, B. (2012). Controls on large-scale patterns of fluvial sandbody distribution in alluvial-to-coastal plain strata: Upper Cretaceous Blackhawk Formation, Wasatch plateau, Central Utah, USA. *Sedimentology*, *59*, 2226–2258.
- Hampson, G. J., Gani, M. R., Sharman, K. E., Irfan, N., & Bracken, B. (2011). Along-strike and down-dip variations in shallow-marine sequence stratigraphic architecture: Upper Cretaceous Star Point Sandstone, Wasatch plateau, Central Utah, USA. *Journal of Sedimentary Research*, *81*, 159–184.
- Hampson, G. J., & Storms, J. E. A. (2003). Geomorphological and sequence stratigraphic variability in wave-dominated, shoreface-shelf parasequences. *Sedimentology*, *50*, 667–701.
- Helland-Hansen, W., & Hampson, G. J. (2009). Trajectory analysis: Concepts and applications. *Basin Research*, *21*, 454–483.
- Helland-Hansen, W., Sømme, T. O., Martinsen, O. J., Lunt, I., & Thurmond, J. (2016). Deciphering Earth's natural hourglasses: Perspectives on source-to-sink analysis. *Journal of Sedimentary Research*, *86*, 1008–1033.
- Hovius, N. (1996). Regular spacing of drainage outlets from linear mountain belts. *Basin Research*, *8*, 29–44.
- Kamola, D. L., & Van Wagoner, J. C. (1995). Stratigraphy and facies architecture of parasequences with examples from the Spring Canyon Member, Blackhawk Formation, Utah. In J. C. Van Wagoner & G. T. Bertram (Eds.), *Sequence stratigraphy of foreland basin deposits: Outcrop and subsurface examples from the Cretaceous of North America* (Vol. 64, pp. 27–54). American Association of Petroleum Geologists, Memoir.
- Kauffman, E. G., & Caldwell, W. G. E. (1993). The Western Interior Basin in space and time. In W. G. E. Caldwell & E.

- G. Kauffman (Eds.), *Evolution of the Western Interior Basin* (Vol. 39, pp. 1–30). Geological Association of Canada, Special Paper.
- Krystinik, L. F., & DeJarnett, B. B. (1995). Lateral variability of sequence stratigraphic framework in the Campanian and lower Maastrichtian of the Western Interior Seaway. In J. C. Van Wagoner & G. T. Bertram (Eds.), *Sequence stratigraphy of foreland basin deposits: Outcrop and subsurface examples from the Cretaceous of North America* (Vol. 64, pp. 11–26). American Association of Petroleum Geologists, Memoir.
- Lawton, T. F. (1986). Fluvial systems of the Upper Cretaceous Mesaverde Group and Paleocene North Horn Formation, central Utah: A record of transition from thin-skinned to thick-skinned deformation in the foreland region. In J. A. Peterson (Ed.), *Paleotectonics and sedimentation in the Rocky Mountain region, United States* (Vol. 41, pp. 423–442). American Association of Petroleum Geologists, Memoir.
- Lawton, T. F., & Bradford, B. A. (2011). Correlation and provenance of Upper Cretaceous (Campanian) fluvial strata, Utah, USA, from zircon U-Pb geochronology and petrography. *Journal of Sedimentary Research*, 81, 495–512.
- Li, Z., & Aschoff, J. (2022). Constraining the effects of dynamic topography on the development of Late Cretaceous Cordilleran foreland basin, western United States. *Geological Society of America Bulletin*, 134, 446–462.
- Liu, S., Nummedal, D., & Gurnis, M. (2014). Dynamic versus flexural controls of Late Cretaceous Western Interior Basin, USA. *Earth and Planetary Science Letters*, 389, 221–229.
- Mahon, R. C., Shaw, J. B., Barnhart, K. R., Hopley, D. E. J., & McElroy, B. (2015). Quantifying the stratigraphic completeness of delta shoreline trajectories. *Journal of Geophysical Research*, 120, 799–817.
- Miall, A. D. (1994). Reconstructing fluvial macroform architecture from two-dimensional outcrops; examples from the Castlegate Sandstone, Book Cliffs, Utah. *Journal of Sedimentary Research*, 64, 146–158.
- Miall, A. D. (2015). Updating uniformitarianism: Stratigraphy as just a set of frozen accidents. In D. G. Smith, R. J. Bailey, P. M. Burgess, & A. J. Fraser (Eds.), *Strata and time: Probing the gaps in our understanding* (Vol. 404, pp. 11–36). Geological Society of London, Special Publications.
- Miller, I. M., Johnson, K. R., Kline, D. E., Nichols, D., & Barclay, R. (2013). A late Campanian flora from the Kaiparowits. In A. L. Titus & M. A. Loewen (Eds.), *At the top of the grand staircase: The Late Cretaceous of Southern Utah* (pp. 107–131). Indiana University Press.
- Milliman, J. D., & Farnsworth, K. L. (2013). *River discharge to the coastal ocean: A global synthesis*. Cambridge University Press.
- Mulder, T., Syvitski, J. P., Migeon, S., Faugetes, J. C., & Savoye, B. (2003). Marine hyperpynal flows: Initiation, behavior and related deposits. A review. *Marine and Petroleum Geology*, 20, 861–882.
- Nyberg, B., Helland-Hansen, W., Gawthorpe, R. L., Sandbakken, P., Eide, C. H., Sømme, T., Hadler-Jacobsen, F., & Leiknes, S. (2018). Revisiting morphological relationships of modern source-to-sink segments as a first-order approach to scale ancient sedimentary systems. *Sedimentary Geology*, 373, 111–133.
- Nyberg, B., Helland-Hansen, W., Tillmanns, F., Gawthorpe, R., & Sandbakken, P. (2021). Assessing first-order BQART estimates for ancient source-to-sink mass budget calculations. *Basin Research*, 33, 2435–2452.
- Parker, L. R. (1976). The paleoecology of the fluvial coal-forming swamps and associated floodplain environments in the Blackhawk formation (Upper Cretaceous) of Central Utah. *Brigham Young University Geological Studies*, 22, 99–116.
- Patrino, S., Hampson, G. J., & Jackson, C. A.-L. (2015). Quantitative characterisation of deltaic and subaqueous clinoforms. *Earth-Science Reviews*, 142, 79–119.
- Patrino, S., & Helland-Hansen, W. (2018). Clinoform systems: Review and dynamic classification scheme for shorelines, subaqueous deltas, shelf edges, and continental margins. *Earth-Science Reviews*, 185, 202–233.
- Pattison, S. A. J. (2019). High resolution linkage of channel-coastal plain and shallow marine facies belts, desert member to Lower Castlegate Sandstone stratigraphic interval, Book Cliffs, Utah–Colorado, USA. *Geological Society of America Bulletin*, 131, 1643–1672.
- Pattison, S. A. J. (2020). Sediment-supply-dominated stratal architectures in a regressively stacked succession of shoreline sand bodies, Campanian Desert member to Lower Castlegate Sandstone interval, Book Cliffs, Utah–Colorado, USA. *Sedimentology*, 67, 390–430.
- Pettit, B. S., Blum, M., Pecha, M., McLean, N., Bartschi, N. C., & Saylor, J. E. (2019). Detrital-zircon U-Pb paleodrainage reconstruction and geochronology of the Campanian Blackhawk–Castlegate succession, Wasatch plateau and Book Cliffs, Utah, USA. *Journal of Sedimentary Research*, 89, 273–292.
- Reineck, H.-E. (1960). Über zeitlücken in rezenten flachseesedimenten. *Geologische Rundschau*, 49, 149–161.
- Romans, B. W., Castellort, S., Covault, J. A., Fildani, A., & Walsh, J. P. (2016). Environmental signal propagation in sedimentary systems across timescales. *Earth-Science Reviews*, 153, 7–29.
- Sadler, P. M. (1981). Sediment accumulation rates and the completeness of stratigraphic sections. *The Journal of Geology*, 89, 569–584.
- Sadler, P. M., & Jerolmack, D. J. (2015). Scaling laws for aggradation, denudation, and progradation rates: The case for timescale invariance at sediment sources and sinks. In D. G. Smith, R. J. Bailey, P. M. Burgess, & A. J. Fraser (Eds.), *Strata and time: Probing the gaps in our understanding* (Vol. 404, pp. 69–88). Geological Society of London, Special Publications.
- Schindel, D. E. (1980). Microstratigraphic sampling and the limits of paleontologic resolution. *Paleobiology*, 6, 408–426.
- Straub, K. M., Duller, R. A., Foreman, B. Z., & Hajek, E. A. (2020). Buffered, incomplete, and shredded: The challenges of reading an imperfect stratigraphic record. *Journal of Geophysical Research: Earth Surface*, 125, e2019JF005079.
- Syvitski, J. P., Peckham, S. D., Hilberman, R., & Mulder, T. (2003). Predicting the terrestrial flux of sediment to the global ocean: A planetary perspective. *Sedimentary Geology*, 162, 5–24.
- Syvitski, J. P. M., & Milliman, J. D. (2007). Geology, geography and humans battle for dominance over the delivery of fluvial sediment to the coastal ocean. *The Journal of Geology*, 115, 1–19.
- Syvitski, J. P. M., Vörösmarty, C. J., Kettner, A. J., & Green, P. (2005). Impact of humans on the flux of terrestrial sediment to the global coastal ocean. *Science*, 308, 376–380.
- Turowski, J. M., Rickenmann, D., & Dadson, S. J. (2010). The partitioning of the total sediment load of a river into suspended

- load and bedload: A review of empirical data. *Sedimentology*, 57, 1126–1146.
- Van Wagoner, J. C. (1995). Sequence stratigraphy and marine to non-marine facies architecture of foreland basin strata, Book Cliffs, Utah, USA. In J. C. Van Wagoner & G. T. Bertram (Eds.), *Sequence stratigraphy of foreland basin deposits: Outcrop and subsurface examples from the Cretaceous of North America* (Vol. 64, pp. 137–223). American Association of Petroleum Geologists, Memoir.
- Wang, Y., Straub, K. M., & Hajek, E. A. (2011). Scale-dependent compensational stacking: An estimate of autogenic time scales in channelized sedimentary deposits. *Geology*, 39, 811–814.
- Yang, Z. S., & Liu, J. P. (2007). A unique Yellow River-derived distal subaqueous delta in the Yellow Sea. *Marine Geology*, 240, 169–176.
- Young, R. G. (1955). Sedimentary facies and intertonguing in the Upper Cretaceous of the Book Cliffs, Utah-Colorado. *Geological Society of America Bulletin*, 66, 177–202.
- Zhang, J., Covault, J., Pyrcz, M., Sharman, G., Carvajal, C., & Milliken, K. (2018). Quantifying sediment supply to continental margins: Application to the Paleogene Wilcox group, Gulf of Mexico. *American Association of Petroleum Geologists Bulletin*, 102, 1685–1702.

**How to cite this article:** Aadland, T., Hampson, G., & Helland-Hansen, W. (2023). A comparison of ancient deltaic shoreline progradation with modern deltaic progradation rates: Unravelling the temporal structure of the shallow-marine Blackhawk Formation, Upper Cretaceous Western Interior Seaway, USA. *Basin Research*, 35, 825–841. <https://doi.org/10.1111/bre.12737>